

Chapter 2

Aspects of the Biology and Physics

Underlying Modified Atmosphere Packaging

Theophanes Solomos

2.1 Introduction

The practice of modified atmosphere packaging (MAP) for fresh and minimally processed refrigerated (MPR) fruits and vegetables is widespread, particularly for commodities with a relatively short storage life (Cameron 1989; Chinnan 1989; Hayakawa et al. 1975; Hobson and Burton 1989; Kader 1986). The subject has been reviewed in the past from both a practical and a theoretical standpoint (Chinnan 1989; Mannapperuma et al. 1991). The beneficial effects of MAP are due in part to the decrease in O₂ and the increase in CO₂ levels, and in part to the decrease in water loss (Ben-Yehoshua et al. 1983; Biale 1946, 1960; Fidler et al. 1973; Isenberg 1979; Kader 1980, 1986; Kidd and West 1945; Lipton and Harris 1974; Smock 1979). In fact, in non-climacteric fruits such as citrus, the prevention of water loss is the main factor contributing to the extension of their storage life (Ben-Yehoshua et al. 1983) (see Chaps. 5, 6 and 7 for packaging materials).

In order to develop an appropriate modified atmosphere (MA) environment, the rates of O₂ uptake and CO₂ evolution, along with the permeability to O₂ and CO₂ of the film, must be known. In addition, the tolerance of the plant materials to the levels of CO₂ and O₂ engendered by MA must also be considered. The optimum levels of O₂ and CO₂ are known for a number of commodities (Fidler et al. 1973; Isenberg 1979; Kader 1985; Saltveit 1989; Smock 1979). In the case of bulky plant organs such as fruits, it is advantageous to determine the diffusivity of O₂ and CO₂ through their skin and flesh in order to avoid the creation of partial anoxia at the center of the tissue as this would be expected to contribute to spoilage and development of off-flavors during extended shelf life periods (Kader 1986).

T. Solomos (✉)

Department of Plant Science and Landscape Architecture, Department of Horticulture,
University of Maryland, College Park, 20742–5011 MD, USA

e-mail: solomost@umd.edu

In this chapter, we discuss aspects of both the biology and physics involved in MAP. We also attempt to address some problems encountered in the generation of non-steady-state predictive models.

2.2 Biological Responses of Plant Tissue to Low O_2 or High CO_2

2.2.1 *Effects of Low O_2 on Senescence of Detached Plant Tissues*

The effects of O_2 on fruit ripening include (1) a diminution in the rate of respiration, (2) a delay in the climacteric onset of the rise in ethylene, and (3) a decrease in the rate of ripening (Blackman 1954; Burg and Burg 1967; Fidler et al. 1973; Kader 1986; Kanellis et al. 1991; Mapson and Robinson 1966; Smock 1979; Solomos 1982; Yang and Chinnan 1988a, b). It was observed by Blackman (1954) that the respiratory isotherms of O_2 uptake as a function of the external O_2 concentration are biphasic in nature in that they include an initial gradual decrease at relatively high O_2 levels, followed by a rapid decline as the levels of O_2 approach zero. The isotherm of CO_2 output follows that of O_2 up to the point where the rate of decline diminishes; in fact, it may even increase as the O_2 level approaches zero (Biale 1960). The rise in CO_2 evolution at low levels of O_2 is obviously caused by the expected Pasteur effect which results in an increase in fermentation. As far as prolonging storage life is concerned, the range of O_2 levels that would be expected to be beneficial must be in the region between the point that induces the initial decline in respiration and that at which it generates partial anoxic environments. It should be underlined that in this region of O_2 levels, the tissue does not experience anoxia because (1) there is no accumulation of ethanol (Table 2.1) and (2) no symptoms of low- O_2 injury develop even after lengthy storage (Fidler et al. 1973; Kader 1986; Loughheed 1987).

Table 2.1 Ethanol content (mM)

Apple no.	Air	Apple no.	1.5% O_2
1	3.294	1	1.32
2	3.422	2	0.56
3	9.264	3	0.09
4	5.361	4	2.18
5	5.584	5	0.54
Avg	5.385	Avg	0.938

“Gala” apples were kept for 180 days in air and 1.5% O_2

Table 2.2 Internal O₂ concentration, rate of respiration, and percentage of V_{max} of oxidases with different $K_m^{O_2}$

Intercellular partial pressure of O ₂ kPa	CO ₂ output (μl·g ⁻¹ ·h ⁻¹)	$K_m^{O_2}$ (μM)				
		0.05	2.2	2.5	3	4
		Percentage of V _{max}				
19.25	5.92	99.98	99.45	99.30	99.10	98.54
6.50	5.90	99.94	99.13	97.52	96.92	95.14
4.91	4.92	99.91	97.47	96.65	95.85	93.52
4.13	4.40	99.90	96.96	95.99	95.03	92.28
2.23	3.34	99.78	93.81	99.91	90.10	85.04
0.92	3.30	98.82	73.60	67.65	62.59	51.11
0.49	2.20	85.63	16.57	12.91	19.65	6.93

The data were calculated from the rate of respiration and diffusion coefficient of O₂ through the skin and flesh of “Gold” apples (Solomos 1987)

The biphasic nature of the O₂ isotherm as a function of external O₂ concentration has been attributed in turn to:

1. The existence of regulatory enzyme(s) that perceive(s) the level of O₂ and exert(s) a feedback inhibition on the initial steps of glucose oxidation, thus lowering respiration (Blackman 1954; Solomos 1982; Tucker and Laties 1985)
2. The effect of resistance to the diffusion of O₂ through the tissue (Chevillotte 1973; James 1953)
3. The presence of a terminal “oxidase” with an affinity for O₂ much smaller than that of cytochrome oxidase (Mapson and Burton 1962)

Work with apples and avocados (Solomos 1982; Tucker and Laties 1985) has shown that suggestion (2) is not a viable explanation of the biphasic nature of the O₂ isotherm. Suggestion (3), that the decrease in respiration at relatively high O₂ levels is due to the presence of an oxidase other than cytochrome oxidase, is difficult to assess. It is fair to say that neither cytochrome oxidase nor the alternative oxidase is expected to be curtailed by the levels of O₂ that initiate a diminution in the rate of respiration. Table 2.2 presents data that indicate that the apparent K_m for O₂ of the putative oxidase must be larger than 4 μM in order to produce an experimentally detectable decrease in CO₂ evolution. It is known that the K_m for O₂ of the cytochrome oxidase is about 0.05 μM, whereas that of the alternative oxidase is 10- to 15-fold higher than that of cytochrome oxidase (Douce 1985; Siedow 1982; Solomos 1977; Tucker and Laties 1985). The data thus preclude the curtailment of either of the known mitochondrial terminal oxidases by relatively high O₂ concentrations. Plant tissues, however, contain terminal “oxidases” that are resistant to the combined inhibition of both cytochrome and alternative oxidase (Laties 1982; Theologis and Laties 1978). Neither the nature of the residual oxidases nor the degree of their participation in plant respiration is known with any degree of precision. Suffice it to say that they are predominantly cytosolic in origin, with rather a low affinity for O₂ (Solomos 1988). Because of this low O₂ affinity, it could be argued that these

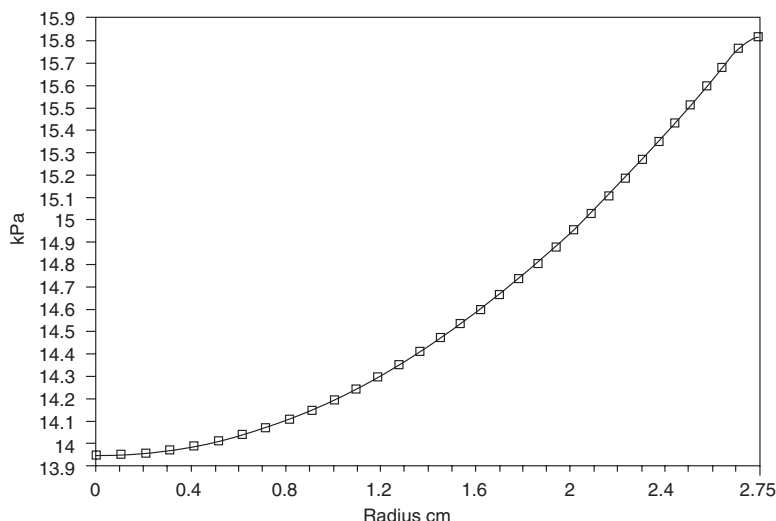


Fig. 2.1 Oxygen distribution along the tuber. The oxygen distribution was calculated from the data concerning the diffusivity of CO_2 in the skin and flesh of potato tubers (Tables 2.11 and 2.12) and the assumption that the sum of the internal partial pressures of CO_2 and O_2 equals the partial pressure of the latter in the ambient atmosphere

“oxidases” may not be contributing to the decrease in respiration with decreasing external O_2 levels. It should be emphasized that in actively respiring plant tissues, such as avocados, the O_2 level is low enough to preclude any appreciable participation of the residual oxidases in the respiration of the fruit. Even in potato tubers, which have much lower rates of respiration than avocado fruits (Solomos and Laties 1976), the oxygen level at the center of the tuber drops to about 13% (Fig. 2.1), a concentration that would be expected to severely curtail the engagement of these “residual” oxidases (Solomos 1988). In addition, their curtailment must exert a feedback restraint on the initial steps of glucose oxidation, yet this is not compatible with the most likely known regulatory mechanisms of plant respiration (Davies 1980; Solomos 1988; Turner and Turner 1980; Wiskich 1980). In the case of climacteric fruits, it may be suggested that the effect of low O_2 on respiration is due to the diminution of ethylene action (Burg and Burg 1967). Therefore, on the basis of the above discussion, it appears that suggestion (1) is the most likely explanation of the effects of low O_2 on fruit respiration.

It was assumed in the past that the accompanying decrease in respiration in response to a lowering of the external O_2 levels was an important facet of the mode of action of low O_2 in prolonging the storage life of fruits (Burton 1974). However, one may argue that the decrease in respiration reflects a metabolic depression engendered by hypoxia. In the first place, hypoxia affects metabolic events in tissues where ripening is not an issue and where ethylene is not involved. For instance, hypoxic conditions inhibited the accumulation of RNA, protein, and DNA synthesis associated with the wounding of potato tubers (Butler et al. 1990). We have also

Table 2.3 Effect of 1.5% O₂ on sugar accumulation and activity of the alternative oxidase in potato tubers stored at 1°C

Days	Sugars ($\mu\text{moles}\cdot\text{g}^{-1}$)			Alternative oxidase nanomoles O ₂ ·min ⁻¹ ·mg protein ⁻¹		
	10 °C Air	1 °C Air	1 °C 1.5% O ₂	10 °C Air	1 °C Air	1 °C 1.5% O ₂
0	16.9	—	—	0.0	—	—
20	19.6	91.5	32.9	0.0	46.63	4.24
30	18.4	113.4	34.4	0.0	60.79	4.16

observed that hypoxia (1.5% O₂) prevented the accumulation of simple sugars and the induction of the alternative oxidase associated with storage of potato tubers at 1 °C (Table 2.3). It should be pointed out that in potatoes, chilling temperatures do not induce the biosynthesis of ethylene. Undoubtedly the delaying effects of low O₂ on the senescence of detached plant organs in general, and fruit ripening in particular, must involve a decrease in ethylene accumulation. In a perceptive paper, Burg and Burg (1967) suggested that the ethylene receptor contains a metal and when it is in its oxidized state, the binding of ethylene is enhanced. However, the effect of hypoxia on ethylene biosynthesis and action may be indirect through the suppressive effects of hypoxia on the induction of 1-amino-cyclopropane-1-carboxylic acid (ACC) synthase and/or synthesis of transducer(s) of ethylene action. It has been reported previously that, in avocados, O₂ concentrations in the range of 2.5–5.5% suppress the activity, appearance of exoenzymes, and accumulation of proteins of cellulose and polygalacturonase, associated with normal ripening (Kanellis et al. 1991). The suppressive effects on the cellulase protein were also reflected in the accumulation of its mRNA. Further, the intensity of inhibition of the synthesis of these hydrolases was inversely related to the levels of O₂ under which the fruits were kept. In addition, the same range of O₂ concentrations that suppressed the synthesis of the hydrolases induced the appearance of anaerobic isoenzymes of alcohol dehydrogenase (ADH). The rates of increase in the levels of cellulose, its mRNA and polygalacturonase, and the disappearance of the anoxic isoenzymes of ADH on reexposure of the fruits to air were directly related to the previous levels of O₂ (Kanellis et al. 1991). The fact that similar ranges of O₂ concentrations on one hand suppressed the rise in the enzymes associated with normal ripening, while at the same time inducing the synthesis of anoxic isoenzymes of ADH, indicates that the O₂ sensing mechanism is common for both processes. The induction of anoxic isoenzymes in response to hypoxia is easily understood because it is advantageous for the tissue to synthesize enzymes that increase the production of ATP in anoxia before oxygen is completely depleted. However, the extension of the storage life of fresh fruits and vegetables must be the consequence of metabolic depression which, unlike anoxia, is not deleterious to the long-term survival of the tissue. Metabolic depression is the most important adaptation for survival of intertidal organisms, which experience frequent transitions from normoxia to hypoxia (Storey and Storey 1990). Because the intensity of respiration could be considered to reflect the intensity

Table 2.4 Days to climacteric under different O₂ concentrations

Year	Harvest date	Treatment					
		Air	8% O ₂	6% O ₂	4% O ₂	3% O ₂	2% O ₂
1987	8–24	19	24	40	66	109	>194
1988	8–26	22	–	–	89	>280	–
1989	8–22	21	–	45	76	103	–
1990	8–24	16	–	–	32	–	105
1991	8–27	9	–	–	–	–	45

of cellular metabolism, and because low oxygen invariably decreases the rate of respiration of such detached plant organs as fruits, flowers, and leaves, this indicates that hypoxia, by an as yet unknown mechanism, produces a decrease in metabolism, which in turn results in diminishing the rate of plant development and hence senescence. In short, the decrease in respiration may not be the cause of the decline in the rate of senescence, but rather a response to a metabolic depression, which diminishes the demand for biological energy.

It has been pointed out that low O₂ in preclimacteric tissues delays the onset of the climacteric rise in ethylene evolution (Mapson and Robinson 1966). Experimental results concerning the range of O₂ concentrations that delay the onset of ripening are limited. It appears that in the case of “Gala” apples, the external O₂ concentration must fall below 8% in order to prolong the preclimacteric stage of the apples (Table 2.4). In short, the system that is involved in the induction of ACC synthase, a key regulatory enzyme in ethylene biosynthesis (Yang and Hoffman 1984), is saturated at O₂ levels above 7–8%. The data of Table 2.4 show, as expected, that the effect of low O₂ on the timing of the onset of ripening differs with the season.

Quantitative data concerning the effect of low O₂ on the rate of ripening are rather difficult to establish. At present it is not possible to describe unequivocally the relationships between O₂ concentration and rate of ripening. Suffice it to say that low O₂ does indeed delay ripening, as has been amply demonstrated in a variety of fruits (Kader 1986; Knee 1980; Kanellis et al. 1991; Liu and Long-Jum 1986; Quazi and Freebairn 1970; Yang and Chinnan 1988a). Yang and Chinnan (1988b) developed a mathematical expression for predicting the changes in the color of tomato fruits as a function of O₂ concentration.

A critical parameter that must be taken into consideration in designing suitable MAP is the limit of O₂ below which the produce cannot be safely stored. This limit, as expected, varies with the produce, but it is important to realize that levels of O₂ that induce partial anaerobiosis will be detrimental to both longevity and quality of the produce. This limit can be assessed experimentally by measuring either the values of the respiratory quotient (RQ) or, preferably, the increase in ethanol content of the tissue. The latter may be a more reliable indicator than the RQ values, especially at levels of O₂ that initiate partial anaerobiosis, and that will be somewhat difficult to detect from the changes in the RQ. Because of its volatility, ethanol can be detected in the ambient atmosphere of MAP by removing a gas sample and determining the ethanol content using gas chromatography (Nakhasi et al. 1991).

2.2.2 *Effects of CO₂ on Senescence of Detached Plant Tissues*

The mode of action of CO₂ on senescence is unclear. Burg and Burg (1967) suggested that CO₂ is a competitive inhibitor of ethylene. Recent experimental evidence indicates that CO₂ may indeed diminish the action of ethylene provided the concentration of the latter is less than 1 $\mu\text{l} \times \text{L}^{-1}$. In the case of apples, CO₂ enhances the inhibitory effects of low O₂ on respiration (Fidler et al. 1973), whereas CO₂ concentrations in the range of 1–27% do not affect the rate of respiration of peaches (Deily and Rizvi 1982). It should be pointed out that CO₂ is a metabolically active molecule participating in a number of carboxylating reactions. In addition, it is expected that high concentrations of CO₂ could alter the pH of the cytosol, which in turn may affect plant metabolism (Siripanich and Kader 1986). Anoxic conditions generated by CO₂ induce changes in a number of intermediate metabolites that differ from those observed when the tissue is kept under nitrogen instead (Kader, personal communication). CO₂ is also required for the action of ACC oxidase (Kuai and Dilley 1992).

It is well known that tolerance to CO₂ varies greatly, not only between species but also between cultivars of the same species. For instance, “Golden Delicious” apples can tolerate high CO₂ concentrations, whereas “McIntosh” apples are damaged by even 3% CO₂ (Fidler et al. 1973). Strawberries can tolerate CO₂ levels as high as 20%, and storage of peaches in 10–15% CO₂ is beneficial (Deily and Rizvi 1982). In apples, high CO₂ concentrations appear to inhibit succinic acid dehydrogenase (Hulme 1956). Storage of lemons under high concentrations of CO₂ leads to an accumulation of organic acids (Biale 1960). In lettuce, high CO₂ concentrations affect the metabolism of phenolic compounds (Siripanich and Kader 1985a, b). Another beneficial effect of high CO₂ levels is their antimicrobial activity. At present it is impossible to predict the tolerance of a particular tissue to high levels of CO₂ (Kader 1986).

2.2.3 *Effects of Slicing on Tissue Metabolism*

The effects of wounding on plant metabolism have been studied extensively in tissues prepared from bulky plant organs such as tubers and roots. The vast literature on this subject has established that slicing induces profound quantitative and qualitative changes in tissue metabolism (Kahl 1974; Laties 1978). The observed changes include a rise in respiration, DNA and RNA synthesis, induction of new enzymes, membrane degradation, and the appearance of novel mRNA (apRees and Beevers 1960; Butler et al. 1990; Clicke and Hackett 1963; Kahl 1974; Laties 1978). The effect of slicing on respiration is probably the most extensively studied aspect of wounding in bulky plant organs (Laties 1978). These investigations have shown that slicing induces a three- to fivefold rise in respiration over that of the parent-plant organ. With aging there is a further two- to threefold increase in respiration (Laties 1978). This rise in respiration with aging of slices is critically dependent on

protein and RNA synthesis since the addition, within 8–10 h of slicing, of either protein or RNA synthesis inhibitors prevents the development of the respiratory rise with aging (Clicke and Hackett 1963; Kahl 1974). Neither the cause of this rise in respiration nor its metabolic significance is clear. However, the data indicate that inhibitors of respiratory development also inhibit a number of biochemical events, such as suberin formation and synthesis of phenolics, associated with aging of potato slices (Kahl 1974; Laties 1978).

Several experiments show that the nature of both respiratory substrates and pathways changes with aging of slices. In particular, in fresh potato slices, most of the respiratory CO_2 is derived from the α -oxidation of fatty acids arising out of the attendant breakdown of phospholipids in response to slicing, whereas carbohydrates are respiratory substrates of aged slices (Jacobson et al. 1970; Laties 1978). It has also been reported that in slices other than potatoes, a large portion of CO_2 is produced by the pentose phosphate pathway (PPP) (apRees and Beevers 1960). In addition it should be mentioned that temperature and gas composition affect both respiratory substrates and pathways. Thus, when potato slices are aged either in air, in the presence of 10% CO_2 , or in a bicarbonate solution, suberin formation is prevented and the tissue develops callus (cf. Laties 1978). Moreover, the respiration of aged slices is manolate resistant and is presumed to comprise the PPP (Kahl 1974). This observation is important from the point of view of MAP because aging in high CO_2 levels may prevent the formation of color in potato slices.

The effects of hypoxia on minimally processed produce, in combination with high CO_2 concentrations, have not been studied in detail. However, based on the observations that hypoxia inhibits the synthesis of DNA, protein, and novel mRNA in potato slices (Butler et al. 1990), it may be anticipated that these conditions repress the synthesis of those enzymes that are considered to exert adverse effects on the quality of tissue slices, for example, phenylalanine ammonia lyase (PAL), this being considered to increase the content of phenolics in the tissue, which in turn tend to increase in wounded plant tissues (Kahl 1974; Uritani and Asahi 1980). In addition MAP environments may suppress the rise in amylases, thus diminishing the breakdown of starch prevalent in potato slices (Kahl 1974).

A number of experimental observations indicate that regardless of the origin of the respiratory reducing equivalents, the terminal electron acceptor is predominantly cytochrome oxidase, even in tissues that possess substantial cyanide-resistant respiration (Laties 1978; Solomos 1988). If this is the case in tissue slices, the oxygen concentration can be reduced to very low levels because of the high affinity for O_2 of the cytochrome oxidase, and because of the short diffusion path available to gases. For instance, in the case of sweet potato slices suspended in air at 25 °C, the rate of O_2 uptake is of zero order with respect to its external concentration until the latter drops to about 0.4% (Fig. 2.2). The ability to decrease the O_2 concentration to such low levels may be beneficial because it is expected to reduce the browning due to polyphenol oxidases (PPO), as the latter have a rather high K_m for O_2 (Beevers 1961).

At present there are no detailed studies concerning the effect of ranges of O_2 and/or CO_2 concentrations on either metabolism, longevity, or quality of cut tissue segments. It is to be expected, as in the case of intact tissues, that O_2 concentrations

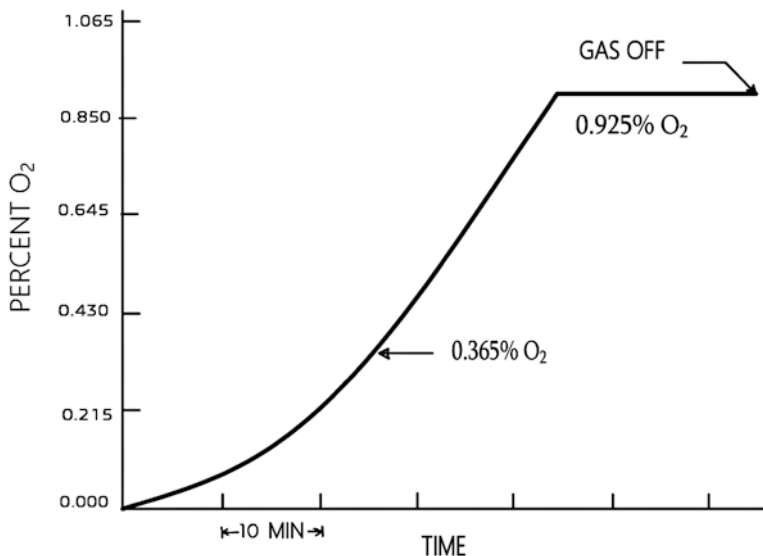


Fig. 2.2 The rate of O₂ uptake of slices suspended in air was followed polarographically. The slices were initially maintained under 0.925% O₂. At the indicated point, the gas was turned off. The rate of O₂ uptake between 20.946% and 0.925% was of zero order

that engender partial anoxia will be detrimental to longevity and quality of the produce. This low limit of O₂ can be assessed in a manner identical to that described earlier for intact tissues.

2.3 Determination of Gas Diffusivities in Plant Tissues

2.3.1 General Considerations

In attempting to generate predictive MAP models, it is useful to know the tissue's permeability to gases in order to calculate their concentration at the center of the organ, particularly when bulky fruits or vegetables are used. The diffusion barriers of a plant organ include the skin, the intercellular spaces, the cell walls, and plasma-lemma. The diffusion of gases through bulky plant organs such as fruits, roots, and tubers follows Fick's first law, and the diffusion channels are predominantly gaseous in nature (Burg and Burg 1965; Burton 1974; Cameron and Yang 1980; Solomos 1987). Simple calculations with apples have shown that, assuming an aqueous diffusion barrier, the maximum radius that could maintain 1% O₂ at the center of the fruit would be about 0.7 cm (Solomos 1987). For fruits with rates of O₂ uptake much larger than that of apples, the radius would be even smaller. Similar observations have also been reported for potato tubers and apples (Burton 1974).

Table 2.5 Relationship between external pressure and internal concentration of C₂H₄

External pressure (kPa)	Internal ethylene concentration (μl)
101.3	472
76	319
37.3	190
25.3	88

From Burg and Burg (1965)

The most convincing evidence for the gaseous nature of the diffusion paths is that provided by Burg and Burg (1965). These authors showed that the diffusivity of gases was inversely related to the external pressure (Table 2.5), as would be expected from the ideal gas law. If the barrier was liquid in nature, the changes in external pressure would not be expected to affect the length of the mean free path because of the incompressibility of water.

Fick's first law states that the flux normal to the surface of a metabolically inert gas is given by (Crank 1970):

$$J = AD \frac{\partial c}{\partial x} \quad (2.1)$$

where J , in $\mu\text{moles sec}^{-1}$ per fruit, is the flux; A , in cm^2 , is the surface available to diffusion; D , in $\text{cm}^2 \text{sec}^{-1}$, is the diffusion coefficient; and $\partial c / \partial x$ is the concentration gradient with respect to distance. It is customary to replace $\partial c / \partial x$ with the difference in concentration $\Delta c / \Delta x$. This is permissible only when the change in concentration with distance is linear (Jacobs 1967; Nobel 1983). In order to determine D , the concentration gradient must first be determined. In the case of non-steady-state conditions, the change in concentration with respect to time should also be known. In order to calculate these gradients, it is necessary to solve the equation for Fick's second law (Crank 1970; Jacobs 1967). The general equation for Fick's second law for a metabolically active gas in three dimensions is (Crank 1970):

$$\frac{\partial c}{\partial t} = D \left[\frac{\partial^2 c}{\partial x^2} + \frac{\partial^2 c}{\partial y^2} + \frac{\partial^2 c}{\partial z^2} \right] \pm v \quad (2.2)$$

where v is the specific rate of evolution (+) or uptake (−) of the gas under consideration. The analytical solutions of Eq. (2.2) are numerous, depending on the boundary conditions and the initial distribution of the gas throughout the barrier. Equations (2.3) and (2.4) below represent the expression of Eq. (2.2) for a solid sphere and cylinder, respectively (Crank 1970; Jacobs 1967):

$$\frac{\partial c}{\partial t} = D \left[\frac{\partial^2 c}{\partial r^2} + \frac{2}{r} \frac{\partial c}{\partial r} \right] \pm v \quad (2.3)$$

$$\frac{\partial c}{\partial t} = D \left[\frac{\partial^2 c}{\partial r^2} + \frac{1}{r} \frac{\partial c}{\partial r} \right] \pm v \quad (2.4)$$

where r , in cm, is the radius of the sphere and cylinder. In cases where the peel of the tissue is the main parameter, these equations must be solved for hollow spherical and cylindrical shells. For nonmetabolic gases, there are analytical solutions for a hollow sphere and cylinder (Crank 1970).

Apart from the mathematical complexities, determining the diffusivity of gases under dynamical conditions introduces a number of uncertainties because of the nonhomogeneous nature of the diffusion barriers of a plant organ. For instance, the diffusion coefficients of CO_2 in the skin and flesh of potato tubers are about 6.90×10^{-7} and $2.50 \times 10^{-4} \text{ cm}^2 \cdot \text{sec}^{-1}$, respectively. The existence of such a barrier in the flesh will generate appreciable concentration gradients within the flesh when the efflux of a gas is measured. To demonstrate this point, it is assumed that CO_2 is diffusing in an infinite cylinder of unit cross-sectional area, with a D_{CO_2} similar to that of potato tuber flesh. Table 2.6 describes the percentage distribution of a quantity M of CO_2 deposited at $x = 0$ and $t = 0$. The change in concentration with time and distance is given by (Crank 1970):

$$C(x,t) = \frac{M}{2\pi(Dt)^{1/2}} \times \exp\left[-\frac{x^2}{4Dt}\right] \tag{2.5}$$

It may be seen from Table 2.6 that the concentration gradient is substantial. Therefore, the assumption that the concentration of a metabolically inert gas is uniform throughout the flesh is not valid (Cameron and Yang 1980).

Another uncertainty of the efflux method is the assumption that the equilibrium between the cellular solution and intercellular spaces is instantaneous. However, a number of observations indicate that this may not be the case. It was shown by Burton (1950) that the evacuation of O_2 from a small plug of potato tissue was a lengthy process. In addition, indirect experimental evidence indicates that the resistance to gas diffusion from the cell to the intercellular spaces may not be negligible (Chevillotte 1973). It is also expected that the solubility of the gas in aqueous solutions would affect the equilibrium distribution between the cell and the intercellular spaces, especially where short time intervals are concerned. A case in point is the changes in RQ in the course of the rapid climacteric rise in respiration. In precli-

Table 2.6 Concentration of CO_2 with distance and time as percent of initial amount deposited at the center of an infinite cylinder with a diffusion coefficient of $2.5 \times 10^{-4} \text{ cm}^2 \cdot \text{sec}^{-1}$

Time (min)	Distance (cm)				
	1	1.5	2	2.5	3
10	12.688	1.370	0.061	0.001	0.000
11	14.223	1.880	0.111	0.003	0.000
15	18.755	4.253	0.533	0.037	0.001
20	21.854	7.182	1.512	0.204	0.018
30	24.009	11.433	4.046	1.064	0.208
40	24.119	13.826	6.344	2.330	0.685
50	23.581	15.109	8.102	3.636	1.365
60	22.843	15.763	9.378	4.809	2.126

macteric avocados, the RQ is close to unity, changes to less than one at the climacteric peak, and then returns toward unity at the postclimacteric stage (Solomos and Laties 1976). It was found, however, that in bananas this pattern of changes was not metabolic in nature, but rather the result of the difference in the respective solubilities of CO₂ and O₂ in water (McMurchie et al. 1972). Because of this difference in solubilities, O₂, which has a smaller solubility in water than does CO₂, equilibrates with the intercellular spaces faster than does CO₂. Further, the efflux method requires a precise knowledge of the volume of the intercellular spaces and the solubility of the gas in the cellular liquid.

However, if appropriate experimental precautions are taken, it may be feasible to obtain reasonable approximations of gas diffusivities through the skin of a plant organ by following the efflux of metabolically inert gases. For instance, if the skin is thin, if the tissue is loaded with relatively high concentrations of the inert gas, if the volume of the vessel is small, and if the diffusion in the flesh is much larger than in the skin, then this method could give reasonable approximations of gas diffusivity through the skin. In order to avoid the generation of the concentration gradient along the flesh of potato tubers, the resistance to diffusion was calculated by considering only the initial linear part of the efflux isotherm of ethane (Banks 1985). This approach, however, introduces some uncertainties concerning the origin of the gas. It was assumed that the gas originated under the skin, which may not be correct because ethane, being nonpolar, is expected to dissolve in the waxy layers of the cuticle. In tissues with thick skin, the volume of the waxy layer can be appreciable. For instance, in a cylindrical tuber of radius 2.8 cm, length 12 cm, and skin thickness 0.012 cm, the volume of the phellem is about 2.5 ml. It is also possible that some of the initial gas efflux may originate from the gas adsorbed on the tuber surface or present in gaseous cavities. This approach could be compared to the ion fluxes, where the initial flux contains a large component of the apparent free space and does not measure fluxes across the cellular membranes, these being the main barrier to ion fluxes between cells and ambient environment (Briggs et al. 1961). It should be emphasized that any determination of gas diffusion is *meaningless* unless it is verified experimentally.

In view of the uncertainties and mathematical complexities involved in the determination of the D of gases under non-steady-state conditions, we shall here consider only steady-state situations.

The steady-state solution of Eq. (2.2), $((\partial c)/\partial t = 0)$, in a one dimensional, plane sheet, for a metabolically active gas is (Hill 1928):

$$C(x) = \frac{v}{2D}x^2 - \frac{\ell v}{D}x + C_0 \quad (2.6)$$

where v , in $\mu\text{moles cm}^{-3}\cdot\text{sec}^{-1}$, is the constant rate of output (+) or uptake (−) of the gas per unit tissue volume; ℓ , in cm, is half of the tissue thickness; and C_0 , in $\mu\text{moles cm}^{-3}$, is the concentration of the gas at $x = 0$, that is, the ambient atmosphere. Thus, the concentrations of CO₂ and O₂ at the center of the tissue C_i are:

$$C_i = C_0 \pm \frac{v}{2D}\ell^2 \quad (2.7)$$

The concentrations of CO₂ and O₂ at the center of a sphere and cylinder are given by Eqs. (2.8) and (2.9), respectively (Hill 1928):

$$C_i = C_0 \pm \frac{v}{6D} R^2 \quad (2.8)$$

$$C_i = C_0 \pm \frac{v}{4D} R^2 \quad (2.9)$$

where R , in cm, is the radius of either the sphere or cylinder. The other notations have been defined earlier.

In the case of metabolically inert hollow spherical and cylindrical shells, the flux of CO₂ per unit time at their surfaces is given by Eqs. (2.10) and (2.11), respectively (Crank 1970):

$$J_{r=R} = 4\pi D \frac{C_i - C_0}{R - R_i} \quad (2.10)$$

$$J_{r=R} = 2\pi Dh \frac{C_i - C_0}{\ln(R/R_i)} \quad (2.11)$$

where R and R_i , in cm, are the outside and inside radii, respectively. In the case of a thin spherical wall (Eq. 2.10), it is assumed that $R \cdot R_i \approx R^2$. The other notations have been defined earlier. It should be pointed out that Eq. (2.11) may not be very accurate unless the surfaces of the cylindrical bases are small in comparison with the cylindrical surface, and the length is much larger than the radius. In the case of oxygen, the order of the concentration differences in Eqs. (2.10) and (2.11) is reversed, for example, $C_0 - C_i$. It is obvious from Eq. (2.11) that for an accurate determination of D , the values of R and R_i must be known with some degree of precision. It is customary to use Eq. (2.12), instead of Eq. (2.11):

$$J_{r=R} = 2\pi rh \frac{C_i - C_0}{\Delta r} D \quad (2.12)$$

and to determine the apparent diffusion coefficient, $D' = (D/\Delta r)$. This could, depending on the dimensions, introduce appreciable error because $D' = R \times (D/\Delta r)$ (Abdul-Baki and Solomos 1994).

Finally the flux of oxygen through a metabolically inert plane sheet is given by Eq. (2.13) (Jacobs 1967):

$$J = \frac{AD(C_0 - C_i)}{\Delta x} \quad (2.13)$$

As already mentioned, gases diffuse in and out of plant organs in gaseous channels. Thus, the usually observed low diffusivities are due to the fact that only a small

fraction of the tissue surface is available to gas diffusion. In “Russet Burbank” potato tubers, the fraction of the surface permeable to gases varies with the tuber from 4.22×10^{-6} to 7.8×10^{-6} , the average being 6.22×10^{-6} (Abdul-Baki and Solomos 1994). It is thus apparent that Eq. (2.1) should be written as:

$$J = ADN \frac{dc}{dx}$$

where N is a number between 0 and unity representing the fraction of the surface that is permeable to gases (Burg and Burg 1965). On the basis of microscopic and gas diffusion measurements, it was calculated that only 1/1000 of the cross section of the flesh of potato tubers is permeable to gases (Woolley 1962).

The diffusivity of gases through plant tissues could also be decreased by the degree of tortuosity of the path. However, in most plant tissues of interest for consumption, the skin is quite thin; hence, the effect of a tortuous path will probably be insignificant.

It was mentioned earlier that for the determination of the diffusion coefficient of the gases for the cases considered above, one must measure the flux and the concentrations of the gases inside and outside the tissue.

2.3.2 Measurements of Intercellular Gases

Several methods have been used in the past to ascertain the internal concentration of gases in various fruits and vegetables. These methods include evacuation, manometric techniques, use of oxygen microelectrodes, and the removal of plugs of tissue which are then sealed in airtight vials (Solomos 1987).

The evacuation technique introduces the following uncertainties. In the first place, the values reflect the overall concentration of the gases in the tissue and not that at a particular point, for example, at the center, under the skin, etc. Further, the evacuated gases will contain not only those present in the intercellular spaces, which is required, but an unknown portion of the dissolved gases in the cellular sap. This in turn requires corrections that must include solubility of gases in the cell liquid and also, depending on time and intensity of respiration, the production or utilization of the gas within the time interval. The use of O_2 microelectrodes has produced measurements of some large O_2 gradients within the tissue (Brädle 1968). Readings of an oxygen microelectrode will vary greatly depending on whether the electrode is submerged in liquid or is in a gaseous phase. The use of manometric techniques, though reliable, requires the construction of special apparatus which makes it difficult to use for a large number of samples (Hulme 1951). Removal of plugs is a destructive method. In addition, it introduces uncertainties in the subsequent analysis of the gases similar to those given above for the evacuation technique.

Banks and Kays (1988) affixed small vials on the surface of potato lenticels and followed the changes in the concentration of CO_2 and O_2 . It is expected that these concentrations in the vials will reflect that under the skin. This method is an

improvement on any of the previous techniques, but the uncertainty exists that the gases may diffuse laterally to adjacent lenticels if the pressure in the vial increases, or the lenticel is partially blocked. Waldraw and Leonard (1939) removed small plugs of tissue to create cavities into which the inserted tubes were in turn sealed airtight. It is anticipated that, with time, the composition of the gas atmospheres of the tubes will equilibrate with the internal gas atmosphere of the tissue. Thus, the composition of the fruit gases can be determined by analyzing the gas in the tubes. Trout et al. (1942) showed that the removal of up to 10 ml of gas from the internal cavity of apple fruit generated no appreciable drop in pressure, and the system returned to equilibrium quite rapidly. However, this may not be the case for plant organs with small intercellular spaces. With improved analytical techniques for measuring gases, a small volume of samples – between 25 and 50 μl – can be used to accurately determine the concentrations of metabolically active gases, that is, O_2 , CO_2 , and C_2H_4 . Several investigators have inserted hypodermic needles into the locule cavities of apple fruits to determine the internal concentration of C_2H_4 (Burg and Burg 1965). The hubs of the needles are sealed with a vaccine cap, and samples are withdrawn from the needle using an airtight syringe. The concentration of C_2H_4 is then measured by gas chromatography (Burg and Burg 1965).

This method can be improved upon further by gluing a chromatographic septum to the calyx of the fruit and inserting the needle through the septum and into the locules (Solomos 1989). This technique facilitates sequential sampling, and the needle can be replaced easily if it becomes blocked. The method has the additional advantage that it inflicts minimal injury, and the needle can be kept in the fruit for longer periods so that the effect of injury is dissipated. In the case of fruits, such as apples, with large locular cavities, the injury effect may not be an issue. Further, because of the small volume of the needle, it is expected that its gas space will come into rapid equilibrium with the intercellular gases, and, in addition, the removal of small volumes of sample gas is expected to represent that in the intercellular spaces adjacent to the needle tip. In this way, gradients across the tissue can be ascertained.

Previous work established, as expected, that the total internal gas pressure equals that of the ambient environment (Hulme 1951; Trout et al. 1942). That requires that the sum of the internal partial pressures of the gases equals the surrounding atmosphere, approximately 1 atm. This is indeed the case for apple fruit (Table 2.7). This in turn suggests that the sampling method does not introduce appreciable experimental error. The rate of gas exchange can be measured either by a static or a flow-through system (Henig and Gilbert 1975; Solomos 1987).

Table 2.7 Internal partial pressure of gases in the atmospheres inside “Gala” apples

	CO_2	O_2	N_2	Total $\text{CO}_2 + \text{O}_2 + \text{N}_2 + \text{argon} + \text{water vapors}$
Experiment 1	0.022	0.181	0.772	1.002*
Experiment 2	0.026	0.183	0.777	1.012
Experiment 3	0.022	0.188	0.777	1.014

*Each reading represents the average of five apples

2.3.3 *Experimental Determination of CO₂ Diffusivity in Apples and Potatoes*

As mentioned above, the diffusion barriers from the cell to the ambient atmosphere include the skin, intercellular spaces, cell walls, and plasmalemma. Most of the previous data were mainly concerned, apart from a couple of exceptions (Burton 1950; Solomos 1987; Woolley 1962), with measuring skin resistance (Banks 1985; Burg and Burg 1965; Cameron and Yang 1980). The main reason for this is that the experimental procedures that were used are not amenable to determining gas diffusion through the intercellular spaces of the flesh. Further, with a few exceptions, the calculated resistances have not been subjected to experimental verification. We shall here briefly describe methods for evaluating gas diffusion coefficients through both skin and flesh, as well as experimental procedures for ascertaining their validity. Here we shall confine the discussion to apples and potato tubers.

2.3.3.1 Apples

We have used varieties of apples whose geometry approaches that of a sphere (Solomos 1987). Within the cultivar, we selected fruits whose equatorial and polar circumferences differed by <5%. In order to subject the data to experimental verification, we altered the rate of CO₂ output by decreasing the external O₂ concentration and comparing the values of CO₂ diffusivities. The experimental arrangements were those described by Burg and Burg (1965), with minor modifications (Solomos 1987, 1989). The geometrical configuration of the skin of the apple was assumed to be a hollow spherical shell. It is apparent from Eq. (2.10) that the concentration of CO₂ under the skin, along with the respiration rates and fruit dimensions, must be known, so that D' can be calculated. The concentration of CO₂ under the skin can be measured by inserting a hypodermic needle just under the surface of the fruit, while the concentration at the center is obtained by inserting a hypodermic needle through the calyx into the locules. In most of the apple cultivars we used, the gradient between the center and the subcutin was quite small (0.2–0.6%) (Solomos 1987). In the case of “Gala,” whose data are presented here, the gradient of CO₂ was between 0.1% and 0.2%, which falls within the experimental error for measuring CO₂. It has been demonstrated that in the case of ethylene, the use of the concentration at the center to represent that under the skin introduced an insignificant error in the values of D' (Solomos 1989). Thus, the concentration of CO₂ under the skin is taken to be identical to that at the center. Table 2.8 shows the diffusion coefficient of CO₂ under different external O₂ concentrations. When the external O₂ concentration was decreased in steps from air to N₂, this of course affected the rate of CO₂ output. It may be seen from Table 2.8 that the diffusivities of CO₂ under different O₂ levels are in reasonable agreement.

Apple fruit pose problems for evaluating the diffusivity of their intercellular spaces. Because of the small difference in CO₂ concentrations between the center

Table 2.8 Diffusion coefficient ($\text{cm}^2\cdot\text{sec}^{-1}\times 10^{-4}$) of CO_2 in the skin of “Gala” apples under different O_2 levels at 15 C

	Apple no.					CO_2 output ($\mu\text{l/G/H}$)
	1	2	3	4	5	
Air	1.67	1.28	1.28	1.50	1.51	6.08
O_2 (13.00%)	1.26	1.17	1.35	1.50	1.30	5.99
O_2 (6.78%)	1.18	0.98	0.99	1.28	1.19	4.29
O_2 (4.75%)	1.18	0.98	0.98	1.28	1.19	4.19
O_2 (1.59%)	1.16	1.48	1.00	1.30	1.47	3.54
O_2 (0.62%)	1.34	1.47	0.94	1.29	1.23	2.91
N_2	1.32	1.20	1.10	1.34	1.32	3.15
AVG	1.301	1.223	1.09	1.356	1.316	
STD	0.164	0.19	0.150	0.093	0.120	

Table 2.9 Diffusion coefficient of CO_2 in the flesh of “Gala” apples

Experiment	$\text{cm}^2\cdot\text{sec}^{-1}\times 10^{-3}$
1	1.46 (0.27)
2	1.47 (1.27)
3	1.26 (0.27)
4	2.13 (0.95)

Each value represents the average of five apples. The number in parentheses is the STD

and subcutin, Eq. (2.8) cannot be used to calculate D . We thus proceeded to peel the fruit, blot it dry with filter paper, and then measure the rate of respiration and internal CO_2 concentration. Within about 6–8 h, the rate of CO_2 evolution was close to that of the intact fruit, probably because the dissolved CO_2 was dissipated. From the rate of CO_2 output and external and internal CO_2 concentrations, its diffusion coefficient in the intercellular spaces was calculated based on Eq. (2.8). The values obtained are presented in Table 2.9. Unfortunately the validity of these values cannot be tested experimentally because with time the outer layers of the fruit will form periderm, thus altering the internal concentration of CO_2 .

2.3.3.2 Potato Tubers

We have used only “Russet Burbank” tubers because their geometry simulates a cylinder. (It should be stressed, however, that no tuber is exactly cylindrical.) The tubers were selected with the proviso that their length be greater than 11 cm and that the circumference, measured at several points along the tuber, not vary by more than 10% (Abdul-Baki and Solomos 1994). The CO_2 concentrations under the skin and at the center were measured by gluing two chromatographic septa, 11 mm in diameter, onto the surface in the middle of the tuber, each septum being 180° apart. Through the septa, two hypodermic needles were inserted, one at the center and the other under the skin. In addition the thickness of the lenticels was measured

microscopically. From the rate of CO₂ output and the concentration of CO₂ under the skin, the diffusion coefficient of CO₂ in the skin was calculated using Eq. (2.11). Table 2.10 shows the values of the D_{CO_2} . It may be seen that there is appreciable variability between the tubers. These values are close to those reported previously for O₂ (Burton 1950). The validity of the data was tested by transferring the tubers from 10 to 27 °C. From the observed values of CO₂ concentration under the skin, and the values of D_{CO_2} calculated from those obtained at 27 °C (Jost 1960), we calculated the rate of CO₂ output at 10 °C and compared it to that observed. The observed and calculated values of respiration are in good agreement (Table 2.11).

Table 2.10 Diffusion coefficient (cm²·sec⁻¹ × 10⁻⁷) of CO₂ in the skin of potato tubers

Tuber no.	10 °C	27 °C
1	7.16	8.21
2	6.73	9.33
3	6.03	6.04
4	6.04	7.97
5	6.37	7.77
6	4.19	5.12
7	5.56	5.98
8	7.79	7.62
Avg	6.24	7.26

The values of D_{CO_2} were calculated by inserting in Eq. (2.11) the observed fluxes and concentrations of CO₂ under the skin and ambient atmosphere, along with dimensions of the tuber and skin thickness (0.012 cm)

Table 2.11 Comparison of observed and calculated rates of CO₂ evolution at 10°C

27 °C	(μmoles·sec ⁻¹ ·10 ⁻²)	
Tuber no.	Observed	Calculated
1	2.97	2.92
2	2.37	1.83
3	2.63	2.96
4	2.34	1.69
5	2.34	1.65
6	2.39	2.20
7	2.56	2.68
8	2.70	2.86
Avg	2.54	2.35

The theoretical fluxes were obtained by inserting in Eq. (2.11) the calculated values of D_{CO_2} at 10 °C from those observed at 27 °C along with the theoretical CO₂ concentration under the skin, calculated as in Table 2.13, the dimensions of the tuber, and the concentration of CO₂ in the ambient atmosphere

Table 2.12 Diffusion coefficient ($\text{cm}^2\cdot\text{sec}^{-1} \times 10^{-4}$) of CO_2 in the flesh of potato tubers

Tuber no.	10 °C	27 °C
1	1.67	1.90
2	2.17	2.23
3	2.63	3.10
4	2.68	2.90
5	2.90	2.46
6	2.30	2.67
7	3.65	3.81
8	1.96	2.10
Avg	2.50	2.65

Table 2.13 Observed and calculated concentrations ($\mu\text{moles}\cdot\text{cm}^{-3}$) of CO_2 under the skin at 10 °C

Tuber no.	Observed	Calculated
1	1.90	1.89
2	1.42	1.51
3	2.66	2.64
4	1.85	1.87
5	1.87	1.86
6	2.93	2.96
7	2.53	2.52
8	2.10	2.10
Avg	2.15	2.17

The theoretical values were obtained by inserting in Eq. (2.9) the calculated values of D_{CO_2} from their value at 27 °C (Jost 1967), along with the observed CO_2 concentration at the center, and the specific respiration

The diffusion coefficient of CO_2 in the flesh was calculated from the values of CO_2 output, based on Eq. (2.9) (Table 2.12). The accuracy of these values was tested by calculating the concentration of CO_2 under the skin from Eq. (2.9) along with the observed concentrations of CO_2 at the center, and the calculated values of D_{CO_2} at 10 °C from the data at 27 °C corrected for temperature (Jost 1960). Here too, the observed and calculated values are in reasonable agreement (Table 2.13).

2.4 Modeling for Appropriate Gas Environment in MAP

2.4.1 General Considerations

MAP is an inexpensive way to generate controlled atmosphere (CA) conditions within the package. The CA environment is generated through the interactions between produce respiration, film permeability to gases, and the ratio between total film area and produce weight. MAP is a dynamic system in that the internal concentration of gases changes continuously until it reaches a steady state, i.e., where the

rates of O_2 and CO_2 fluxes equal their respective rates of utilization and production. Modeling thus includes a determination of the time it takes for the gases to reach their steady-state levels, which must equal their desired concentrations for the produce under consideration. However, the non-steady-state part of the modeling is of limited practical value and may be ignored. Modeling can be carried out under steady-state conditions.

At any time, the rate of changes in the concentrations of O_2 and CO_2 per unit volume of free gas space in the package can be expressed as:

$$\frac{d[O_2]}{dt} = \frac{P_{O_2} A \{ [O_2]_{out} - [O_2]_{in} \}}{V} - \frac{R_{O_2} W}{V} \quad (2.14)$$

$$\frac{d[CO_2]}{dt} = \frac{-P_{CO_2} A \{ [CO_2]_{in} - [CO_2]_{out} \}}{V} + \frac{R_{O_2} W}{V} \quad (2.15)$$

where $[O_2]$ and $[CO_2]$, in ml/cm^3 , are the concentrations of O_2 and CO_2 , respectively; P_{O_2} and P_{CO_2} , in $ml/h \text{ cm}^2 \text{ ml cm}^{-3}$, are the permeabilities of the film to O_2 and CO_2 ; A , in cm^2 , is the area of the film; R_{O_2} and R_{CO_2} , in $ml \text{ kg}^{-1}/h^{-1}$, are the rates of O_2 uptake and CO_2 output, respectively; W , in kg , is the weight of the produce; and V , in cm^3 , is the free gaseous volume of the package (void volume).

Obviously when the system reaches steady state, the changes in CO_2 and O_2 concentrations in the package with time are zero; hence,

$$R_{O_2} W = P_{O_2} A \{ [O_2]_{out} - [O_2]_{in} \} \quad (2.16)$$

$$R_{CO_2} W = P_{CO_2} A \{ [CO_2]_{in} - [CO_2]_{out} \} \quad (2.17)$$

2.4.2 Rate of Respiration

The solutions of Eqs. (2.14) and (2.15) require a precise knowledge of the rates of O_2 uptake and CO_2 evolution, which in turn vary with the concentrations of O_2 and CO_2 , that is, $R_{O_2} = f(O_2, CO_2)$ and $R_{CO_2} = g(O_2, CO_2)$. Further, the effect of O_2 or CO_2 on the rate of respiration is also dependent on the stage of maturity. For instance, in preclimacteric “Gala” apples, the rate of CO_2 output decreases when the external O_2 concentration drops below 8.10 kPa (8%), whereas in the climacteric kind, the rate of CO_2 output is of zero order with respect to the external O_2 concentration up to 2.53 kPa (2.5%) (unpublished observations). The rates of O_2 uptake and CO_2 output can be determined using a flow-through system. Here, a stream of gas is passed through the tissue which is enclosed in a jar. The levels of O_2 and CO_2 in the outlet stream are monitored. This method is probably the most accurate. However, it is not practicable to measure the rate of respiration under a number of combinations

of O_2 and CO_2 . Alternatively, the tissue may be enclosed in a vessel, and the changes in O_2 and CO_2 in the head space can be measured. At any instant, the change in the concentrations of O_2 and CO_2 will be dependent on the rate of respiration, the volume of the gas space in the vessel, and the weight of the tissue. Therefore,

$$R_{O_2} = \frac{V_0}{W} \frac{d[O_2]}{dt} \quad (2.18)$$

This method has the advantage that the rate of respiration can be determined under a variety of O_2 and CO_2 concentrations. However, if rapid changes in the rate of respiration are involved, they could introduce some uncertainty, especially with bulky plant organs, because of the large differences between the solubilities of O_2 and CO_2 in water. It is thus expected that the external O_2 levels will reach equilibrium between the concentrations in the intercellular gas spaces and the ambient atmosphere faster than will those of CO_2 . It has been noted earlier that this can introduce appreciable experimental error in the values of RQ. Nevertheless, if appropriate ratios of the volume of the respiratory vessel to weight of tissue are chosen, it is possible that the concentration of gases in the ambient and fruit atmospheres will be close to equilibrium because the changes occur gradually. A number of authors have determined the rate of O_2 uptake by scrubbing the CO_2 in the vessel (Cameron et al. 1989; Henig and Gilbert 1975). Because of the absorption of CO_2 , the pressure of the jar will decrease with time. This may introduce some experimental errors because of possible contamination from air during the withdrawal and subsequent injection of the gas into the gas chromatogram. Cameron (1989) measured the rate of O_2 depletion by enclosing an O_2 electrode in the jar, thus eliminating this source of experimental error.

Once the relationship between rates of O_2 uptake and CO_2 output as a function of both O_2 and CO_2 levels is determined, an expression is generated by various interpolation techniques. A number of interpolation methods have been used in the past to express the rates of O_2 uptake and CO_2 output as a function of O_2 and CO_2 concentrations. Henig and Gilbert (1975) divided the isotherms showing the percentage of gas versus time into linear and curvilinear segments. The latter part was plotted on semilog arithmetic paper, and both segments were subjected to regression analysis for the determination of the coefficients and intercepts. Hayakawa et al. (1975) expressed the rate of respiration in stepwise linear segments which were subsequently used to develop a predictive MAP model. Cameron (1989) fitted the O_2 depletion data to an exponential function, whereas Yang and Chinnan (1987, 1988a) used polynomial interpolations.

Unfortunately previously published modeling work was mainly concerned with intact tissue. There is a scarcity of experimental data regarding both the optimal MAP conditions and the effects of O_2 and CO_2 on the rate of respiration of tissue segments.

As mentioned above, slicing of tissues cut from such plant organs as tubers and roots invokes an immediate two- to fourfold increase in respiration over the parent organs (Laties 1978). In addition, there is a further two- to threefold increase with aging.

The latter increment depends on temperature and on whether the aging takes place with slices that are submerged in aerated liquid or in moist air (cf. Laties 1978). The facts that (1) slice respiration is mediated mainly by cytochrome oxidase with a K_m for O_2 of 0.05 μM (Solomos 1988; Theologis and Laties 1978) and (2) the resistance to diffusion through the flesh is lower than that through the skin indicate that tissue slices at relatively low temperatures can be maintained at quite low O_2 concentrations. For instance, the diffusion of O_2 in potato flesh is about $2.9 \times 10^{-4} \text{ cm}^2 \text{ sec}^{-1}$ (Table 2.11). If it is assumed that at 10 °C the rate of O_2 uptake is 9 $\mu l \text{ kg}^{-1} \text{ h}^{-1}$, and the ambient O_2 concentration is 2%, then the O_2 level at the center of a slice 2 cm thick will be about 0.4%, which will result in a 6.7 μM O_2 solution in the adjacent cells, a concentration that is unlikely to limit cytochrome oxidase. We have observed that the rate of O_2 uptake of sweet potato slices 2 mm thick at 25 °C is of zero order with respect to its external level until the latter decreases below 0.5% (Fig. 2.2).

The effect of temperature on MAP modeling must also be considered because it affects both the rate of respiration and film permeability to gases. The effects of temperature on plant respiration can be expressed as Arrhenius-type equations (James 1953). In chilling-sensitive tissues, there is an increase in the energy of activation at low temperatures (Lyons 1973). Further, in a number of tissues, low temperatures may induce a rise in respiration. A classic example is potato tubers, where storage at 1 °C evokes a rise in respiration above that observed at 10 °C (Isherwood 1973).

Changes in the permeability of gases through the film with temperature can also be expressed by an Arrhenius-type equation (Mannapperuma et al. 1991). The authors have determined the energy of activation of a number of commercially available films.

2.4.3 Steady-State Modeling

The most important aspect of MAP modeling is the design of suitable packaging for generating the requisite gas environment for long-term storage of the commodity. Usually, the establishment of the steady-state CA environment takes about 24 h, which is adequate for most commodities. In cases where the creation of the desired gas composition has to be accelerated, the package can be flushed with the appropriate gas mixture before sealing. It should be underlined that the time for the system to reach its final steady state is determined by the parameters that are used for the creation of the long-term desired gas composition. A detailed knowledge of the transient changes in the gas composition is of limited practical value, though very interesting from a theoretical point of view.

It has been noted above that under steady-state conditions, the concentrations of O_2 and CO_2 inside the package can be considered constant, although small changes occur gradually due to changes in the respiratory activity of the tissue under the new gas environment. Thus, $(d[O_2]_{in}/dt)$ and $(d[CO_2]_{in}/dt)$ are zero, and the equilibrium fluxes can be determined from Eqs. (2.16) and (2.17). It is apparent from these equations that the internal concentrations of O_2 and CO_2 will be determined from the rates

of O_2 uptake and CO_2 evolution, weight of the tissue, and area and permeability properties of the film. Combining Eqs. (2.16) and (2.17) we obtain:

$$\frac{R_{O_2}}{R_{CO_2}} = \frac{P_{O_2}}{P_{CO_2}} \frac{[O_2]_{out} - [O_2]_{in}}{[CO_2]_{in} - [CO_2]_{out}} \quad (2.19)$$

It is evident that both the RQ and the ratio of permeabilities of O_2 over CO_2 will be critical in establishing a particular CA environment. For most tissues, RQ is close to one, in particular for tissue slices of bulky plant organs such as tubers and roots (Laties 1978). Assuming a value for RQ of 1, Eq. (2.18) can be rearranged to become:

$$[CO_2]_{in} = \frac{P_{O_2}}{P_{CO_2}} [O_2]_{out} + [CO_2]_{out} - \frac{P_{O_2}}{P_{CO_2}} [O_2]_{in} \quad (2.20)$$

A plot of $[O_2]_{in}$ against $[CO_2]_{in}$ will result in a straight line with a slope equal to the permeability ratio, as $[CO_2]_{out}$ can be neglected, and the $P_{O_2} / P_{CO_2} \cdot [O_2]_{out}$ is constant. Figure 2.3 illustrates the relationship between $[O_2]_{in}$ and $[CO_2]_{out}$ for 1/2, 1/4, 1/5, and 1/6 permeability ratios of O_2 over CO_2 . These ratios were chosen because they are the most common in commercially available films. For a successful MAP package, the combination of internal concentrations of O_2 and CO_2 will fall close to the line for a given permeability ratio.

Equations (2.16) and (2.17) show that the area of the film, along with the weight of the tissue, will be critical in establishing a desired MAP environment. If W/A is denoted by ρ , then:

$$[O_2]_{in} = [O_2]_{out} - \frac{R_{O_2}}{P_{O_2}} \rho \quad (2.21)$$

$$[CO_2]_{in} = [CO_2]_{out} + \frac{R_{CO_2}}{P_{CO_2}} \rho \quad (2.22)$$

In this way, an appropriate W/A ratio can be selected to move the internal CO_2 and O_2 concentrations toward the point where the lines of Fig. 2.3 intersect the right-hand y-axis.

Jurin and Karel (1963) determined the steady-state internal oxygen concentration from the intercept of the plot of the experimental rates of respiration and flux across the film as a function of O_2 concentration. Cameron (1989) and Cameron et al. (1989) fitted the curve showing oxygen depletion versus time to an exponential equation:

$$[O_2] = a \left[1 - e^{-(b/c)^d} \right] \quad (2.23)$$

where a , b , and c are constants. The rate of respiration at steady state was calculated by multiplying the time derivative of Eq. (2.23) by the V/W ratio, where V , in lit, and

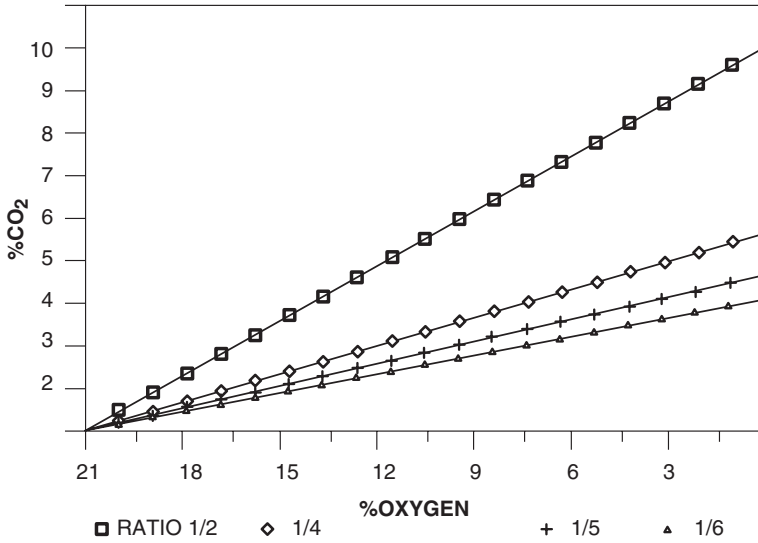


Fig. 2.3 Steady-state relationship between the internal concentrations of CO_2 and O_2

W , in kg, are the void volume of the vessel and weight of tomato fruits, respectively. The transient changes were ignored; only steady-state modeling was considered. It should be noted that Eq. (2.23) may not always be appropriate to use with plastic bags because of the changes in the void volume due to film shrinkage. Changes in V are produced by the decrease in the internal pressure due to differences in the permeabilities of O_2 and CO_2 . This necessitates a decrease in volume so that the internal total gas pressure equals the ambient pressure (see later). Equations (2.16) and (2.17) are more appropriate because the volume is not a variable.

In summary, for modeling an appropriate MAP package, first the desired concentration of gases for a particular commodity can be selected from the compilation of previous data (Isenberg 1979; Kader 1985; Saltveit 1989). Then from the values of respiration under the chosen MAP environment, the appropriate film and $W/A(\rho)$ ratio can be determined.

2.4.4 Dynamic Modeling

Non-steady-state modeling can predict both the time from the start until the virtual steady-state is established, and the steady-state concentrations of O_2 and CO_2 in the package. In order to generate the appropriate expressions, the equations expressing the rate of respiration as $f(\text{O}_2, \text{CO}_2)$ must be inserted into Eqs. (2.14) and (2.15). The results in the literature differ somewhat (Chinnan 1989; Hayakawa et al. 1975; Mannapperuma et al. 1991). These differences could be partly biological in nature

because of the inherent variability in biological material, and because of the limited number of determinations that are usually used. The differences could also be due to physical considerations in assessing the rate of respiration and changes in gas concentrations inside the package during the transient stage.

In order to illustrate the latter point, we assume a solid sphere with a diffusion coefficient similar to that for O_2 in the “Russet Burbank” potato tuber ($2.94 \times 10^{-4} \text{ cm}^2 \text{ sec}^{-1}$). Further, at zero time, the sphere contains no O_2 and is transferred to a vessel where the O_2 concentration is maintained constant at $9.1 \text{ } \mu\text{moles cm}^{-3}$ O_2 (air concentration at 10°C). It is also assumed that oxygen is not utilized by the tissue. It can be shown that for boundary conditions $C(R, t) = C_0$, $t > 0$, and $C(0, t) = 0$ for $0 < t < t_2$, and initial conditions $C(r, 0) = 0$, the solution of Eq. (2.2) is:

$$C(r, t) = C_0 + \frac{2RC_0}{\pi r} \sum_{n=1}^{\infty} \frac{(-1)^n}{n} \sin \frac{n\pi r}{R} \cdot \exp\left(-\frac{n^2 \pi^2}{R^2} \cdot Dt\right) \quad (2.24)$$

where C_0 , in $\mu\text{moles} \cdot \text{cm}^{-3}$, is the concentration of O_2 in the ambient atmosphere; R , in cm, is the radius of the sphere; t , in sec, is the time; and D , in $\text{cm}^2 \text{ sec}^{-1}$, is the diffusion coefficient. It may be seen from Fig. 2.4a and b that even after 10 min, the concentration of O_2 at $r = 1$ is almost zero. Figure 2.4b demonstrates the distribution of O_2 along the radius after 1 h. It should be noted that the gradient would have been steeper if the utilization of O_2 had been incorporated into the solution of Eq. (2.2) and if the resistance to O_2 diffusion of the skin had also been included. Even if the initial O_2 distribution is not zero, the concentration gradient could be appreciable (Crank 1970).

It is likely that under rapid changes in the external O_2 concentration in a closed system, an appreciable concentration gradient of oxygen along the organ will develop. Under these conditions, the rate of respiration of the cells on the periphery will differ from those at the center of the organ because of the substantial differences in O_2 concentration. Further, the changes in respiration calculated from the gas isotherms may represent part of the respiration of the organ, because the distribution of the cells at the center may not be perceived.

It has been noted above that because of the differences in O_2 and CO_2 permeabilities through the film, a partial vacuum is generated inside the package which in turn produces a decrease in void volume in order that the internal pressure may equal the ambient pressure. In short, the void volume is also a function of time, and Eq. (2.14) should be written as follows:

$$\frac{d[O_2]}{dt} = \frac{P_{O_2} A \{ [O_2]_{\text{out}} - [O_2]_{\text{in}} \}}{Vt} - \frac{R_{O_2} W}{V(t)} \quad (2.25)$$

A note of caution is also appropriate regarding the global validity of the rates of respiration calculated from the gas isotherms. In general, a number of interpolations produce a unique function. This, however, may not be the case for all methods of interpolation (Lancaster and Salkauskas 1986). Although the uniqueness of the local expression may be assured, this may not necessarily reflect the biochemical

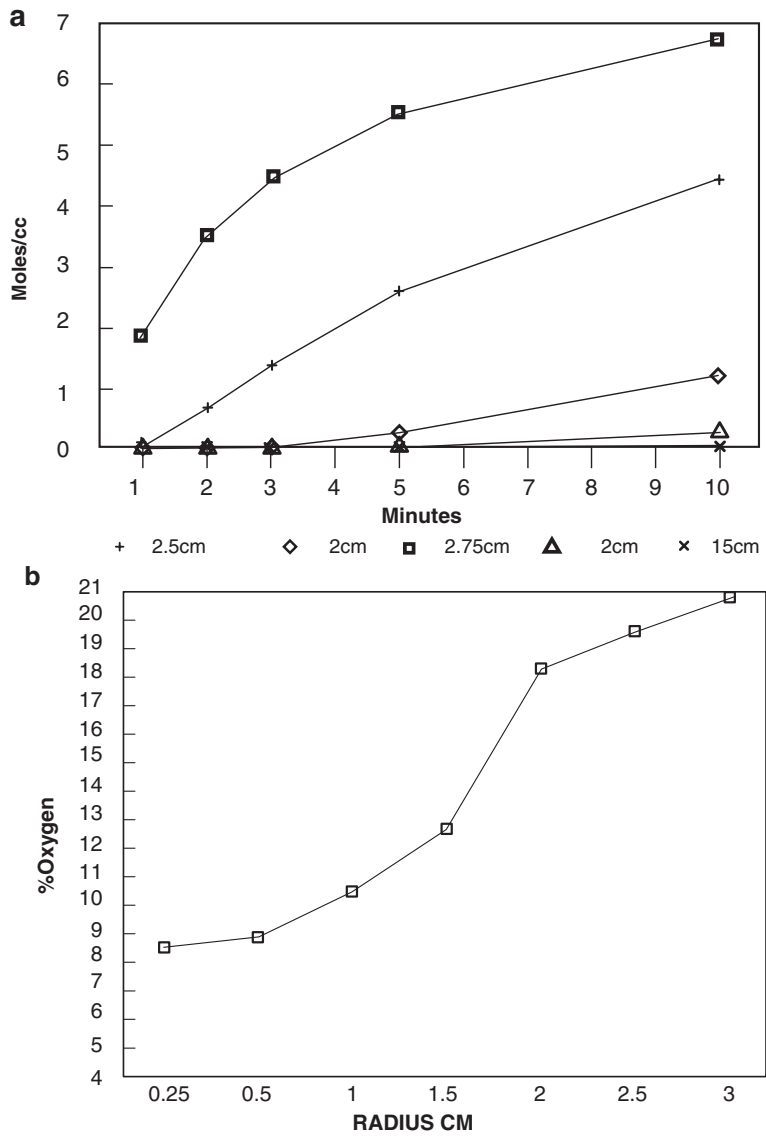


Fig. 2.4 The distribution of oxygen along the radius of a sphere with a diffusion coefficient similar to that in potato flesh. (a) Changes with time in O_2 concentration at a number of points along the radius. (b) Distribution of oxygen across the sphere after 1 h. O_2 at zero time was 0%

behavior of the system. For instance, the rate of respiration of a number of plant tissues is of zero order at concentrations of O_2 from 15% to 100% (Burton 1974; James 1953; Tucker and Laties 1985). If the local expressions reflected the biochemical events that underly plant respiration, the extension of the interpolation

to concentrations of O_2 larger than those in air will result in respiration being independent of O_2 .

It should also be noted that the relationship between O_2 and respiration is enzymatic in nature and may involve more than one terminal oxidase whose affinities for oxygen may differ. Furthermore, the suppression of respiration may be the result of a metabolic depression involving alterations in the kinetic properties and/or amount of key regulatory respiratory enzymes (Storey and Storey 1990). It may thus be more appropriate to develop mathematical expressions reflecting the kinetics of multienzyme sequences (Goldbeter 1991) rather than the usual interpolating techniques that are frequently used in the literature.

2.4.4.1 Experimental Dynamic MAP Modeling

The literature on dynamic MAP modeling has been reviewed previously (Chinnan 1989; Mannapperuma et al. 1991). Here a limited amount of previous research, representing different approaches to deriving predictive mathematical expressions, will be considered.

Deily and Rizvi (1982) produced analytical formulae for predicting the gas concentration and the time necessary to reach the final dynamic equilibrium for peach fruits. They observed that the O_2 depletion isotherm consists of linear and exponential segments with an inflection point at about 5% O_2 and 20% CO_2 . Further, the rate of respiration was unaffected by CO_2 concentrations in the range of 1–27%. Since the optimal MAP environment for peach storage was found to be 10–15% O_2 and 15–25% CO_2 , and since the rate of respiration is constant under these conditions, the authors solved Eqs. (2.14) and (2.15) for constant R_{O_2} and R_{CO_2} . The analytical formulae derived for calculating O_2 and CO_2 are:

$$y(t) = \bar{y} + (y_a - \bar{y}) \cdot \exp(-AP_{O_2} t / V) \quad (2.26)$$

$$z(t) = \bar{z} + (z_a - \bar{z}) \cdot \exp(-AP_{CO_2} t / v) \quad (2.27)$$

where \bar{y} and \bar{z} are the steady-state levels of O_2 and CO_2 , calculated from the steady-state solution of Eqs. (2.14) and (2.15) and from limit $(y(t)/t \rightarrow \infty)$. y_a and z_a are the internal concentrations of O_2 and CO_2 at $t = 0$. The analytical formulae were tested by comparing the experimental and predicted gas concentrations using different films. Table 2.14 shows a good agreement between observed and calculated values.

Henig and Gilbert (1975) solved Eqs. (2.14) and (2.15) numerically using the experimental results of the respiration rate as a function of external O_2 and CO_2 concentrations. The authors validated the computer modeling with the experimental data. The experimental results with a FV-71 film package were in good agreement with the computer-predicted results (Fig. 2.5) (Henig and Gilbert (1975)). The authors also tested the validity of the computer model by altering the variables of the inputs, for example, permeability, weight/void volume ratio, and film area. Their results

Table 2.14 Parameters and results of analytical and experimental determination of model packages of peach fruits

Parameters	Package types		Film overlaps on foam trays		
	Bags	Super-L-bags	Super firm	Barrier bag	Polyolefin
W	0.21	212.30	0.32	0.23	0.31
R_y	7.84	7.84	7.84	7.84	7.84
R_z	7.55	7.55	7.55	7.55	7.55
S	0.12	0.11	0.04	0.04	0.03
V	2.34	2.32	533.90	439.60	614.00
K_y	166.67	166.67	166.67	0.10	0.06
K_z	200.00	200.00	200.00	5.54	0.29
$\hat{y}(\%)$	12.48	11.92	—	—	—
$\hat{z}(\%)$	6.62	7.05	—	—	—
t	96.00	108.00	20.00	10.00	10.00
Analyt					
$O_2\%$	15.99	15.55			
$CO_2\%$	4.12	4.61			

W , S , and V are the weight, surface, and void volume of the package, respectively. R_y and R_z are the rates of O_2 uptake and CO_2 output, respectively, and K_y and K_z are the permeabilities to O_2 and CO_2 , respectively, of the films. \hat{y} and \hat{z} are the steady-state levels of O_2 and CO_2 , respectively. t = time after packaging (h)
From Deily and Rizvi (1982)

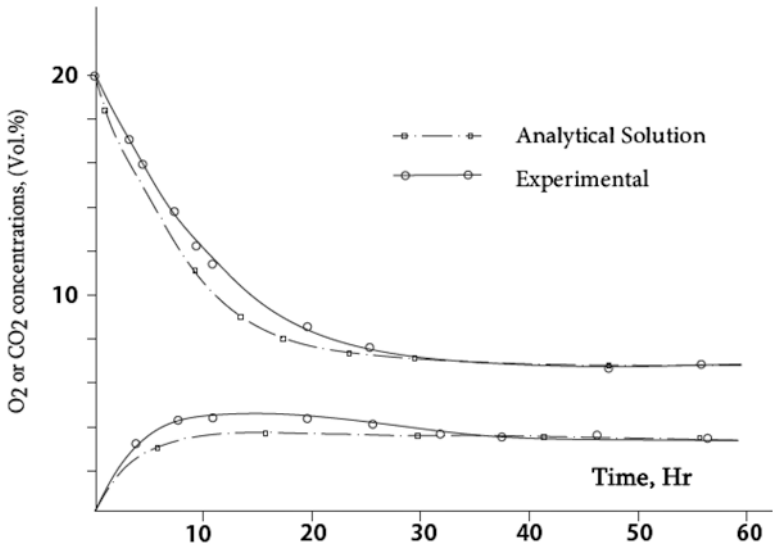


Fig. 2.5 Changes with time in O_2 and CO_2 concentrations in a RMF-61 film package of tomato fruits (From Henig and Gilbert 1975)

showed that the predicted steady-state values of CO_2 and O_2 concentrations were similar to those expected.

Hayakawa et al. (1975) derived an analytical solution of Eqs. (2.14) and (2.15) using Laplace transforms. The rate of respiration was expressed as linear segments:

$$R_{\text{O}_2} = a_i [\text{O}_2] + p_i [\text{CO}_2] + q_i \quad (2.28)$$

$$R_{\text{CO}_2} = d_i [\text{O}_2] + e_i [\text{CO}_2] + f_i \quad (2.29)$$

where a_i , p_i , q_i , d_i , e_i , and f_i are constants, and $[\text{O}_2]$ and $[\text{CO}_2]$ are the analytical expressions determining the O_2 and CO_2 levels. Because of computational complications, the authors assumed that the rate of O_2 uptake of tomato fruits was not critically affected by CO_2 ; hence, $p_i = 0$. Similarly it was assumed that the rate of CO_2 output was not significantly affected by the external O_2 levels. There is some uncertainty concerning the latter assumption because usually the rate of CO_2 evolution parallels that of O_2 uptake as a function of external O_2 concentrations up to the inflection point. Nevertheless, the predicted transient changes in O_2 and CO_2 concentrations were similar to those observed experimentally (Fig. 2.6).

Yang and Chinnan (1987) measured the rates of O_2 uptake and CO_2 output under 20 combinations of external O_2 and CO_2 concentrations. These data were subsequently used to develop a computer-predictive model by expressing the rates of O_2 uptake and CO_2 output as a second-degree polynomial of O_2 , CO_2 , and time (Yang and Chinnan 1988a):

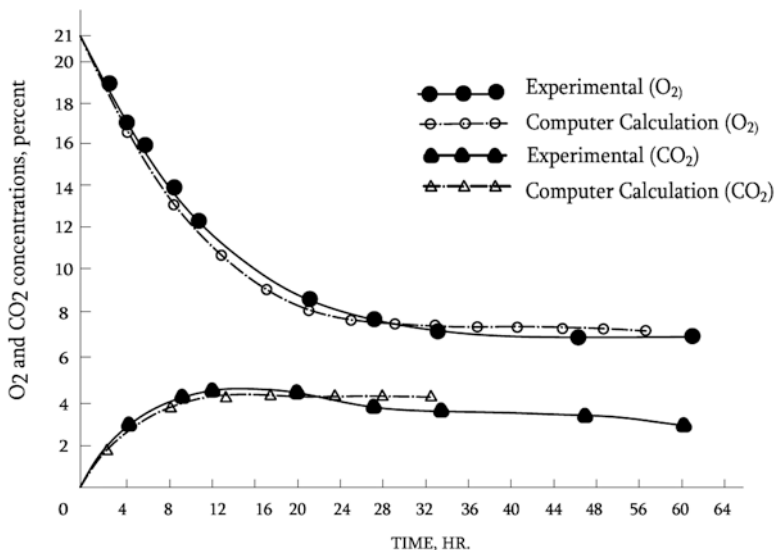


Fig. 2.6 A comparison between experimental and computed O_2 and CO_2 concentrations in a RMF-61 film package of tomato fruits (From Hayakawa et al. 1975)

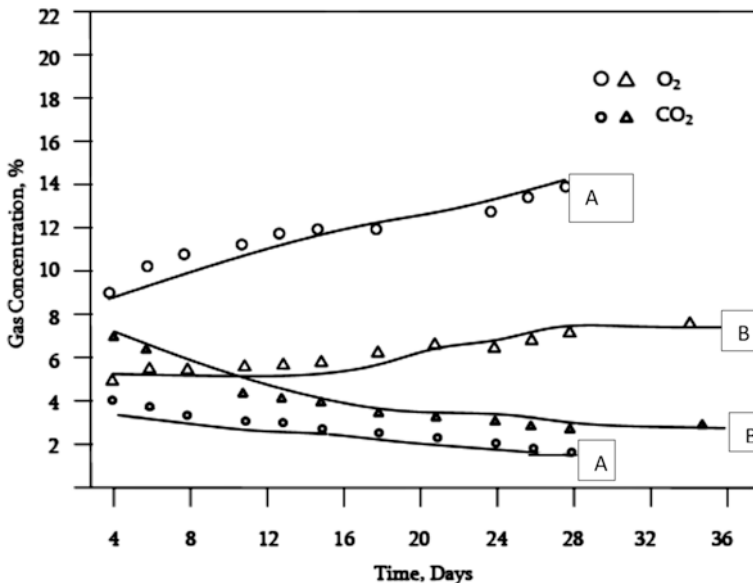


Fig. 2.7 A comparison between experimental (○△●▲) and computed (—) results of the atmosphere in two packages (A and B) made from cryo-pack E-type film. Both packages had the same surface area (1392 cm²). Packages A and B contained two and four tomatoes, respectively (From Yang and Chinnan 1988b)

$$R_{O_2} = a_0 + a_1 C_o + a_2 C_c + a_3 t + a_4 C_o^2 + a_5 C_c^2 + a_6 t^2 + a_7 C_o C_c + a_8 C_o t + a_9 C_c t \quad (2.30)$$

where C_o and C_c are the concentrations of O₂ and CO₂, respectively, and $a_0 \dots a_9$ are constants. The calculated values were tested by comparing them with the experimental observations at two arbitrary combinations of O₂ and CO₂ levels (Fig. 2.7). The prediction of the steady-state concentrations of O₂ and CO₂ was achieved by iterative techniques which minimize the sum of the squares of the O₂ and CO₂ fluxes at short time intervals as the system approaches steady state (Yang and Chinnan 1988b). An innovative aspect of this work is the development of expressions to predict quality attributes, such as color, as a function of O₂ and CO₂. This is very useful for determining the apparent K_m for O₂ of the enzyme(s) whose activity is restricted by O₂, thus producing a slowing of metabolic reactions in plant senescence in general and fruit ripening in particular.

2.5 Effects of Hypoxia on Plant Tissues

Hypoxia affects a large number of metabolic activities in plant tissues, for example, the induction and suppression of gene expression (Bailey-Serres and Chang 2005; Geigenberger 2003; Giovannoni 2004; Klok et al. 2002; Liu et al. 2005; van Dongen

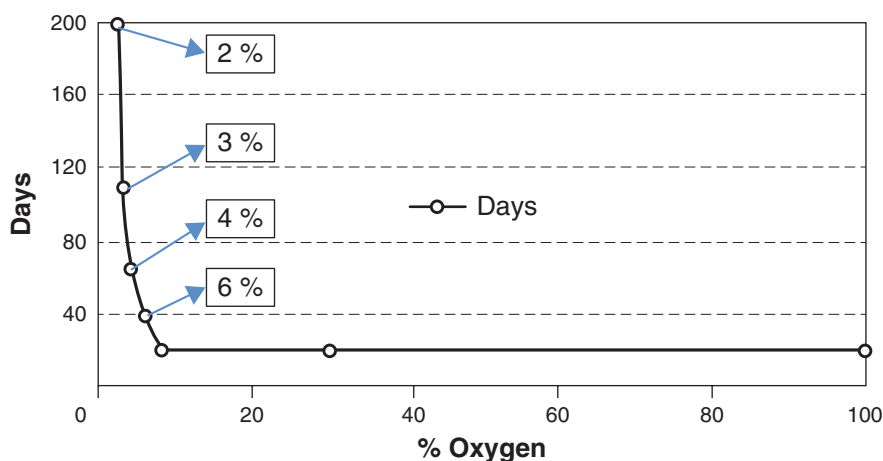


Fig. 2.8 Effect of hypoxia on the timing of the C_2H_4 climacteric onset in “Gala” apples

et al. 2009). Genes induced by hypoxia include anoxic proteins such as ADH (Kanellis et al. 1990). Conversely, hypoxia also suppresses the synthesis of existing proteins, such as those involved in cell wall synthesis, e.g., cellulase and polygalacturonase. In climacteric fruit ripening in general, its most profound effect lies in its suppression of the induction of the C_2H_4 onset. In apples, for example, the delay of the climacteric onset is initiated when the oxygen concentration falls below 8% (Fig. 2.8). Obviously, the effects of hypoxia are saturable with respect to oxygen.

2.6 Concluding Remarks

Substantial progress has been made in our understanding of the molecular aspects underlying the beneficial effects of low O_2 and/or high CO_2 on the shelf life of plant tissues. These include the induction of a number of genes as well as the suppression of the genes involved in the synthesis of existing proteins. At present, however, work still remains to be done regarding the nature of genes that are suppressed by hypoxia. This work will in turn shed light on the molecular aspects of the beneficial effects of MAP on plant tissues.

References

- Abdul-Baki AA, Solomos T (1994) Diffusivity of carbon dioxide through the skin and flesh of ‘Russet Burbank’ potato tubers. *J Am Soc Hort Sci* 119:742–746
- apRees T, Beevers H (1960) Pentose phosphate pathway as a major component of induced respiration of carrot and potato slices. *Plant Physiol* 35:839–847

- Bailey-Serres J, Chang R (2005) Sensing and signaling in response to oxygen deprivation in plants and other organs. *Ann Bot (Lond)* 96:507–518
- Banks NH (1985) Estimating skin resistance to gas diffusion in apples and potatoes. *J Exp Bot* 36:1842–1850
- Banks NH, Kays SJ (1988) Measuring internal gases and lenticel resistance to gas diffusion in potato tubers. *J Am Soc Hort Sci* 113:577–580
- Beevers H (1961) Plant respiration. Row, Paterson and Co., New York
- Ben-Yehoshua S, Shapiro B, Even-Chen Z, Lurie S (1983) Mode of action of plastic film in extending life of lemon and bell pepper fruits by alleviation of water stress. *Plant Physiol* 73:87–93
- Biale JB (1946) Effect of oxygen concentration on respiration of avocado fruit. *Am J Bot* 33:363–373
- Biale JB (1960) Respiration of fruits. In: Wolf J (ed) *Handbuch der Plantenphysiologie. Encyclopedia of plant physiology*, vol X11/2. Springer, Berlin, pp 536–592
- Blackman FF (1954) Analytical studies in plant respiration. Cambridge University Press, London
- Brädle R (1968) Die Verteilung der Sauerstoffkonzentrationen in fleischigen Speicherorganen (Apfel, Bananen, Kartoffelknollen). *Ber Schweiz Bot Ges* 78:330–364
- Briggs GE, Hope AB, Robertson RN (1961) Electrolytes and plant cells. Blackwell Scientific Publications, Oxford
- Burg SP, Burg EA (1965) Gas exchange in fruits. *Physiol Plant* 18:870–886
- Burg SP, Burg EA (1967) Molecular requirements for the biological activity of ethylene. *Plant Physiol* 42:144–151
- Burton WG (1950) Studies on the dormancy and sprouting of potatoes. I The oxygen content of potato tuber. *New Phytol* 49:121–134
- Burton WG (1974) Some biophysical principles underlying the controlled atmosphere storage of plant material. *Ann Appl Biol* 78:149–168
- Butler W, Cook C, Vaya ME (1990) Hypoxic stress inhibits multiple aspects of potato tuber wound process. *Plant Physiol* 93:264–270
- Cameron AC (1989) Modified atmosphere packaging: a novel approach for optimizing package oxygen and carbon dioxide. In: *Controlled Atmosphere Research Conference*, Wenatchee, WA
- Cameron AC, Yang SF (1980) A simple method for the determination of resistance to gas diffusion in plant organs. *Plant Physiol* 70:21–23
- Cameron AC, Boylan-Pett WE, Lee J (1989) Design of modified atmosphere systems. Modeling oxygen concentrations within sealed packages of tomato fruits. *J Food Sci* 54(1413–1416):1421
- Chevillotte P (1973) Relation between the reaction of cytochrome oxidase-oxygen uptake in cells *in vivo*. The role of diffusion. *J Theor Biol* 39:277–295
- Chinnan MS (1989) Modeling gaseous environment and physio-chemical changes of fresh fruits and vegetables in modified atmospheric storage. *American Chemical Society Symposium*, pp 189–202
- Clicke RE, Hackett DP (1963) The role of protein and nucleic acid synthesis in the development of respiration in potato tuber slices. *Proc Natl Acad Sci U S A* 50:243–250
- Crank J (1970) The mathematics of diffusion. Clarendon Press, Oxford
- Davies DD (1980) Aerobic production of organic acids. In: Davies DD (ed) *The biochemistry of plants. A comprehensive treatise*, vol 2. Academic, New York, pp 581–611
- Deily KR, Rizvi SSH (1982) Optimization of parameters for packaging of fresh peaches in polymeric films. *J Food Process Eng* 5:23–41
- Douce R (1985) Plant Mitochondria. Academic, New York
- Fidler JC, Wilkinson BG, Edney KL, Sharples RO (1973) The biology of apple and pear storage. Research Review. No. 3. Commonwealth Bureau of Horticulture and Plant Crops. East Malling, Maidstone, Kent
- Geigenberger P (2003) Response of plant metabolism to too little oxygen. *Curr Opin Plant Biol* 6:247–256
- Giovannoni JJ (2004) Genetic regulation of fruit development and ripening. *Plant Cell* 16(Supplement):S170–S180

- Goldbeter A (1991) Models for oscillation and excitability in biochemical systems. In: Biological kinetics. Cambridge University Press, Cambridge, pp 107–154
- Hayakawa KI, Henig YS, Gilbert SG (1975) Formulae for predicting gas exchange of fresh produce in polymer film package. *J Food Sci* 40:186–191
- Henig YS, Gilbert SG (1975) Computer analysis of the variables affecting respiration and quality in produce packaged in polymeric films. *J Food Sci* 40:1033–1035
- Hill AV (1928) Diffusion of oxygen and lactic acid through tissues. *Proc R Soc Biol Ser B* 104:39–96
- Hobson G, Burton KS (1989) The application of plastic film technology to the preservation of fresh horticultural produce. *Prof Hort* 3:20–23
- Hulme AC (1951) Apparatus for the measurement of gaseous conditions inside apple fruits. *J Exp Bot* 2:65–85
- Hulme AC (1956) Carbon dioxide injury and the presence of succinic acid in apples. *Nature* 178:218
- Isenberg MFR (1979) Controlled atmosphere storage of vegetables. *Hort Rev* 1:337–394
- Isherwood AC (1973) Starch-sugar interconversion in *Solanum tuberosum*. *Phytochemistry* 12:2579–2591
- Jacobs MH (1967) Diffusion processes. Springer, New York
- Jacobson BS, Smith B, Epstein S, Laties GG (1970) The prevalence of carbon-13 in respiratory carbon dioxide as an indicator of the type of endogenous substrate. *J Gen Physiol* 25:1–17
- James WO (1953) Plant respiration. Oxford University Press, Oxford
- Jost W (1960) Diffusion in solids, liquids and gases. Academic, New York
- Jost W (1967) Physical chemistry, an advanced treatise, Eyring H, Henderson D, Jost W. (eds) Academic, New York
- Jurin V, Karel M (1963) Studies on control of respiration of McIntosh apples by packaging methods. *Food Technol* 17:104–108
- Kader AA (1980) Prevention of ripening in fruits by use of controlled atmospheres. *Food Technol* 34:51–54
- Kader AA (1985) Modified atmospheres: an index reference list with emphasis on horticultural commodities. Post Harvest Hort Series 3(Supplement No. 4), University of California, Davis
- Kader AA (1986) Biochemical and physiological basis for effects of controlled and modified atmospheres on fruits and vegetables. *Food Technol* 40:94–104
- Kahl G (1974) Metabolism in plant storage tissue slices. *Bot Rev* 40:263–314
- Kanellis AK, Solomos T, Roubelakis-Angelakis KA (1990) Suppression of cellulase and polygalacturonase and induction of alcohol dehydrogenase isoenzymes in avocado fruit mesocarp subjected to low oxygen stress. *Plant Physiol* 96:269–274
- Kidd F, West C (1945) Respiratory activity and duration of life of apples. *Plant Physiol* 20:467–504
- Klok EJ, Wilson IW, Wilson D, Chapman SC, Ewing RM, Somerville SC, Peacock WJ, Dolferus R, Dennis ES (2002) Expression profile analysis of the low-oxygen response in *Arabidopsis* root cultures. *Plant Cell* 14:2481–2494
- Knee M (1980) Physiological responses of apple fruits to oxygen concentrations. *Ann Appl Biol* 96:243–253
- Kuai J, Dille DR (1992) Extraction, partial purification and characterization of L-aminocyclopropane-L-carboxylic oxidase from apple fruit. *Postharvest Biol Technol* 1:203–211
- Lancaster P, Salkauskas K (1986) Curve and surface fitting. Academic, New York
- Laties GG (1978) The development and control of respiratory pathways in slices of plant storage organs. In: Kahl G (ed) Biochemistry of wounded plant tissues. Walter de Gruyter, Berlin, pp 421–466
- Laties GG (1982) The cyanide-resistant, alternative path in higher plant respiration. *Annu Rev Plant Phys* 33:519–555
- Lipton WJ, Harris CM (1974) Controlled atmosphere effects for fresh vegetables and fruits: why and when. In: Haard NF, Salunke DK (eds) Postharvest biology and handling of fruits and vegetables, vol 2. AVI Publishing, Westport, CT

- Liu FW, Long-Jum C (1986) Responses of daminozide-sprayed McIntosh apples to various concentrations of oxygen and ethylene in simulated CA storage. *J Am Soc Hort Sci* 111:400–403
- Liu F, VanToai T, Moy LP, Bock G, Linford LD, Quackenbush J (2005) Global transcription profiling reveals comprehensive insights into hypoxic response in *Arabidopsis*. *Plant Physiol* 137:1115–1129
- Lougheed EC (1987) Interactions of oxygen, carbon dioxide, temperature and ethylene that may induce injuries in vegetables. *HortScience* 22:791–794
- Lyons SM (1973) Chilling injuries in plants. *Annu Rev Plant Physiol* 24:445–446
- Mannapperuma JD, Singh RP, Montero ME (1991) Simultaneous gas diffusion and chemical reaction in foods stored in modified atmospheres. *J Food Eng* 14:167–183
- Mapson LW, Burton WG (1962) The terminal oxidases of potato tuber. *Biochem J* 82:19–25
- Mapson LW, Robinson JE (1966) Relation between oxygen tension, biosynthesis of ethylene, respiration and ripening changes in banana fruit. *J Food Technol* 1:215–225
- McMurchie EJ, McGlasson BW, Eaks JL (1972) Treatment of fruit with propylene gives information about the biogenesis of ethylene. *Nature* 237:235–236
- Nakhasi S, Schlimme D, Solomos T (1991) Storage potential of tomatoes harvested at the breaker stage using modified atmosphere packaging. *J Food Sci* 55:55–59
- Nobel PS (1983) *Biophysical plant physiology*. Freeman and Company, San Francisco
- Quazi MH, Freebairn HT (1970) The influence of ethylene, oxygen and carbon dioxide on ripening of bananas. *Bot Gaz* 131:5–14
- Saltveit ME (1989) A summary of requirements and recommendations for the controlled and modified atmosphere storage of harvested vegetables. In: *Controlled Atmosphere Research Conference*, Wenatchee, WA
- Siedow JN (1982) The nature of cyanide-resistant pathway in plant mitochondria. *Rec Adv Phytochem* 16:47–84
- Siripanich J, Kader AA (1985a) Effects of CO₂ on total phenolics, phenyl-alanine ammonia lyase, and polyphenol oxidase in lettuce tissue. *J Am Soc Hort Sci* 110:249–253
- Siripanich J, Kader AA (1985b) Effects of CO₂ on cinnamic acid 4-hydroxylase in relation to phenolic metabolism in lettuce tissue. *J Am Soc Hort Sci* 110:333–335
- Siripanich J, Kader AA (1986) Changes in cytoplasmic and vacuolar pH in harvested lettuce tissue as influenced by CO₂. *J Am Soc Hort Sci* 111:73–77
- Smock RM (1979) Controlled atmosphere storage of fruits. *Hort Rev* 1:301–336
- Solomos T (1977) Cyanide-resistant respiration in higher plants. *Annu Rev Plant Physiol* 28:279–297
- Solomos T (1982) Effect of oxygen concentration on fruit respiration: nature of respiratory diminution. In: Richardson DG, Meheriuk M (eds) *Controlled atmospheres for storage transport of perishable agricultural commodities*. Timber Press, Beaverton, OR, pp 161–170
- Solomos T (1987) Principles of gas exchange in bulky plant tissues. *HortSci* 22:766–771
- Solomos T (1988) Respiration in senescing plant organs: its nature, regulation, and significance. In: Nooden LD, Leopold AC (eds) *Senescence and aging in plants*. Academic, New York
- Solomos T (1989) A simple method for determining the diffusivity of ethylene in ‘McIntosh’ apples. *Sci Hortic* 39:311–318
- Solomos T, Laties GG (1976) Effects of cyanide and ethylene on respiration of cyanide-sensitive and cyanide-resistant plant tissues. *Plant Physiol* 58:47–50
- Storey KD, Storey JM (1990) Metabolic rate depression and biochemical adaptation in anaerobiosis, hibernation and estivation. *Q Rev Biol* 65:145–174
- Theologis A, Laties GG (1978) Relative contribution of cytochrome-mediated and cyanide-resistant electron transport in fresh and aged potato slices. *Plant Physiol* 62:238–242
- Trout SA, Hall EG, Robertson RN, Hackney FMV, Sykes SM (1942) Studies in the metabolism of apples: preliminary investigations on internal gas composition and its relation to changes in stored ‘Granny Smith’ apples. *Aust J Exp Biol Med Sci* 20:219–231
- Tucker M, Laties GG (1985) The dual role of oxygen in avocado fruit respiration: kinetic analysis and computer modeling of diffusion-affected respiratory oxygen isotherms. *Plant Cell Environ* 8:117–127

- Turner JS, Turner DH (1980) The regulation of glycolysis and pentose pathway. In: Davies DD (ed) The biochemistry of plants: a comprehensive treatise, vol 2. Academic, New York, pp 279–316
- Uritani I, Asahi T (1980) Respiration and related metabolic activity in wounded and infected plant tissues. In: Davies DD (ed) The biochemistry of plants: a comprehensive treatise, vol 2. Academic, New York, pp 463–485
- van Dongen JT, Fröhlich A, Ramirez-Aguillar SJ, Schauer N, Fernie AR, Erban A, Kopka J, Clark J, Langer A, Geigenberger P (2009) Transcript and metabolite profiling of the adaptive response to mild decreases in oxygen concentration in the roots of *Arabidopsis* plants. *Ann Bot (Lond)* 103:269–280
- Waldraw CW, Leonard ER (1939) Studies on tropical fruits: IV. Methods in the investigation of respiration with special reference to banana. *Ann Bot* 3:27–42
- Wiskich JT (1980) Control of the Krebs cycle. In: Davies DD (ed) The biochemistry of plants. A comprehensive treatise, vol 2. Academic, New York, pp 243–278
- Woolley JT (1962) Potato tuber tissue respiration and ventilation. *Plant Physiol* 37:793–798
- Yang CC, Chinnan MS (1987) Modeling of color development of tomatoes in modified atmosphere storage. *Trans ASABE* 30:548–553
- Yang CC, Chinnan MS (1988a) Modeling of the effect of CO₂ on respiration and quality of stored tomatoes. *Trans ASABE* 31:920–925
- Yang CC, Chinnan MS (1988b) Computer modeling and color development of tomatoes stored in polymeric film. *J Food Sci* 53:869–872
- Yang SF, Hoffman NE (1984) Ethylene biosynthesis and its regulation. *Annu Rev Plant Physiol* 35:155–189

Minimally Processed Refrigerated Fruits and Vegetables

Yildiz, F.; Wiley, R.C. (Eds.)

2017, XXI, 774 p. 186 illus., 122 illus. in color.,

Hardcover

ISBN: 978-1-4939-7016-2